Review Article

On the use of a constant phase element (CPE) in electrochemistry

Samantha Michelle Gateman[1], Oumaïma Gharbi[2],
Hercílio Gomes de Melo[3], Kieu Ngo[2], Mirelle Turmine[2] and
Vincent Vivier[2]

Abstract
Several techniques can be used to experimentally determine the interfacial capacitance of an electrode, which is a crucial parameter used for quantifying the efficiency of super-capacitors. However, the values obtained from cyclic voltam-metry can be significantly different from those extracted from electrochemical impedance spectroscopy analysis. This is particularly due to the fact that the interface does not behave like an ideal (i.e., frequency independent) capacitor, and re-quires the adoption of a constant phase element (CPE). In this article, we present the state of the art on this apparent differ-ence and on the error that can result from one or the other technique using CPE analysis.

Addresses
[1] Department of Chemistry, The University of Western Ontario, London, ON, Canada
[2] Sorbonne Université, CNRS, Laboratoire de Réactivité de Surface, Paris, France
[3] Departamento de Engenharia Metalúrgica e de Materiais, Escola Politécnica da Universidade de São Paulo, Av. Professor Mello Moraes, 2463, São Paulo, SP, Brazil

Corresponding author: Vivier, Vincent (vincent.vivier@sorbonne-universite.fr)

Keywords
Impedance spectroscopy, Cyclic voltammetry, Constant-phase element, Double layer, Electrochemistry, Supercapacitor.

Introduction

Although electrochemistry is a well-established disci-pline, the description of the metal/electrode interface and the resulting interfacial capacitance are still important topics of discussion, as evidenced by some recent articles [1—3]. In the case of an ideally polarizable electrode, the electrochemical interface consists in a capacitive-like behavior accounting for the electrical double layer (EDL) as well as the possible presence of a thin oxide film that may form at the electrode's surface [4]. Discussions about the determi-nation of the capacitance depending on the method used have been already reported in the literature [5—7]. In practice, the measured capacitance depends on the frequency, and to account for such behavior, a constant phase element (CPE) is often assumed/used during analysis of electrochemical impedance spectroscopy (EIS) instead of a pure capacitor [8,9]. Despite its controversial use for several decades [10—12], there exists a point of agreement that the use of a CPE re-flects the real misunderstanding of the electrical behavior of the solid/liquid interface. Although the CPE is now a widely spread electrical element implemented for the analysis of experimental EIS results, only a few works implementing cyclic voltammetry are making use of this element [13—15]. Indeed, the analysis of voltammograms is most often performed assuming a perfect capacitance, which does not depend on the po-larization potential of the electrode. Yet, the capacitance can be a function of the scan rate [14—17]. This can, therefore, lead to significant uncertainty in the deter-mination of extracted capacitance values from cyclic voltammetry, which is generally the technique used for investigating electrochemical supercapacitors.

In this article, we present how capacitance measure-ments obtained by cyclic voltammetry and EIS can differ significantly even though they aim to measure the same physical quantity. Indeed, discrepancies arise because electrochemical impedance spectroscopy measures solely the differential capacitance, whereas both differential capacitance or integral capacitance and/can be derived from cyclic voltammetry (CV) experiment, and more importantly, the CPE behavior is often omitted when analyzing CV curves. A compre-hensive discussion based on the analysis of the seminal equations describing the electrical properties of the interface is first presented, followed by addressing recent works that attempt to correlate the results ob-tained by these two techniques.

Figure 1
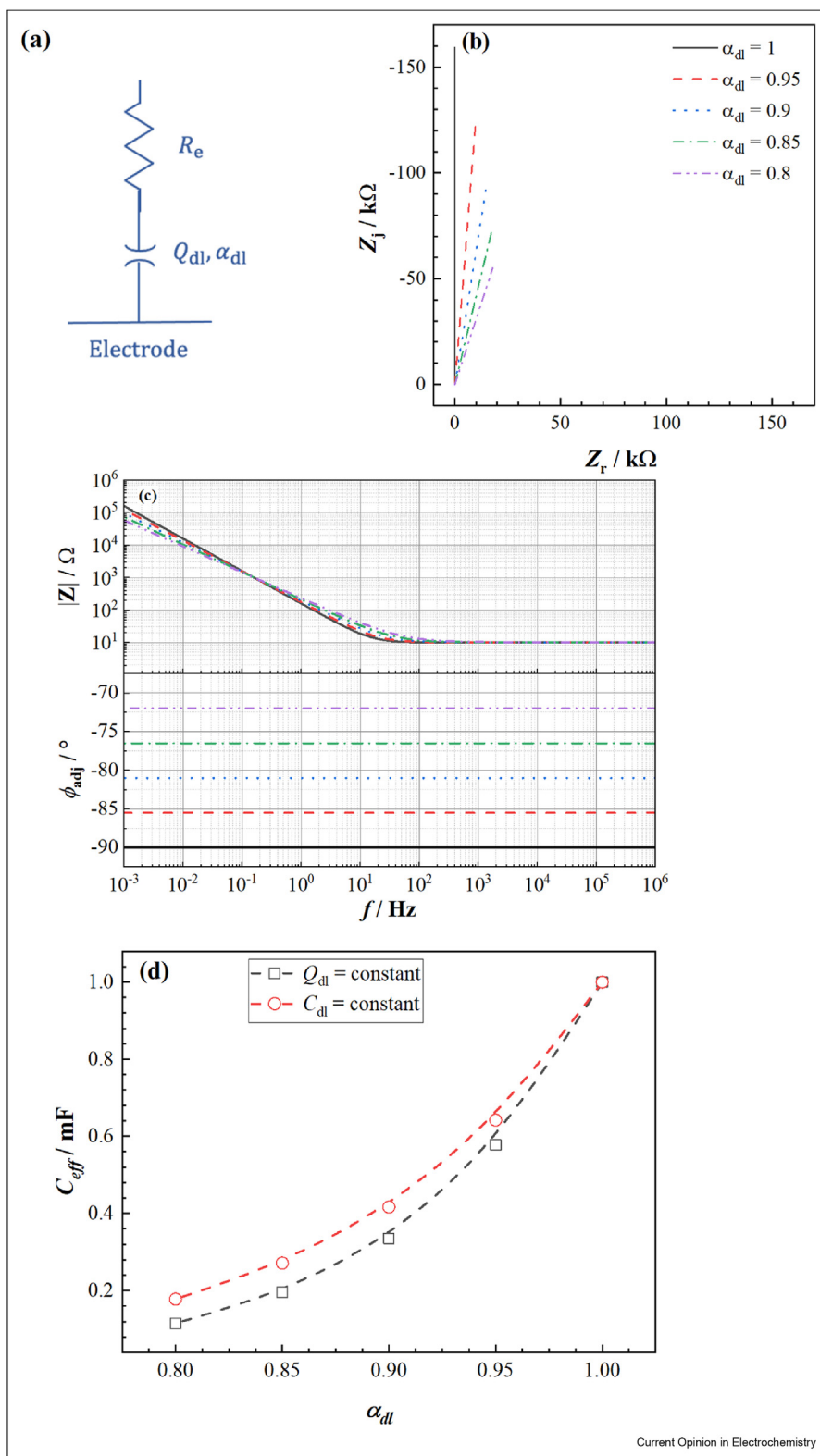
(a) Equivalent circuit commonly used for describing an ideally polarizable electrode; (b) Nyquist diagrams of simulated EIS response for a pure capacitive behavior and for different value of α_{dl} ($Q_{dl} = 1\ mFs^{(\alpha_{dl}-1)}$, $R_e = 10\ \Omega$); (c) Bode representation of the EIS diagrams simulated in (b); (d) Effective capacitance determined on the EIS diagrams presented in (black squares) and assuming a constant value of C_{dl} using the Brug's formula for calculating Q_{dl} (red circles).

Definition of a CPE

The CPE originates from a distribution of time constants that were explained by the dispersion of solution resistance, R_e, and/or the dispersion of the interfacial capacitance, C_{dl}. Regardless of the origin of the CPE, its experimental observation has been reported in all fields of electrochemistry, including corrosion [18,19] and corrosion protection [20−22], batteries [23−27], supercapacitors [28] and solar cells [29], and chemical or biochemical sensors [30,31], and it was shown that the direct use of RC circuit may lead to poor estimation of the electric double layer capacitance [32].

The impedance of a CPE is given by Eq. (1):

$$Z_{CPE}(\omega) = \frac{1}{(j\omega)^{\alpha_{dl}} Q_{dl}}$$

Eq. 1

where, Q_{dl} and α_{dl} are the parameters defining the CPE. In this relation, α_{dl} is a dimensionless parameter comprised between 0 and 1, and Q_{dl} expresses in $Fs^{(\alpha_{dl}-1)}cm^{-2}$. When $\alpha_{dl} = 1$, the system behaves as a pure capacitor, whereas when α_{dl} is smaller than 0.6, it is appropriate to wonder about the origin of this dispersion and its representation in the form of a CPE. When α_{dl} belongs to the 0.6−1, the shape of the impedance diagrams is significantly distorted: the Nyquist representation of the impedance of a CPE (Equation (1)) is a straight line forming an angle of $90 \times \alpha_{dl}$ degrees with the x-axis, whereas if the CPE is in parallel with a resistance (i.e., a charge transfer resistance), then the time constant is a semi-circle more or less flattened depending on the value of α_{dl}.

The analysis of this formula shows the stumbling blocks between the mathematical tools that allow to fit experimental results and a physical interpretation of this behavior [10,11,33,34]. Indeed, the dimensional analysis of the equation shows that a CPE is not a capacity, and that the direct use of the parameters Q_{dl} and α_{dl} is in general not possible without a comprehensive understanding of the interfacial properties [35−37].

Figure 1a show the electrical equivalent circuit suited for the description of an ideally polarizable electrode. It consists of a CPE that accounts for the EDL and the solution resistance, providing a convenient electrical description of the interface of supercapacitors.

CPE in the time domain

As CPEs are widely used for fitting experimental EIS data by means of electrical equivalent circuits, their use can also be extended to analyze cyclic voltammetry experiments, especially for investigation of supercapacitor materials. The consequence of the CPE behavior for the time domain is translated, from a mathematical point of view, by a fractional partial differential equation, which is expressed as Eq. 2

$$i_c(t) = Q_{dl} \frac{d^{\alpha_{dl}} V(t)}{dt^{\alpha_{dl}}}$$

Eq. 2

where, i_c is the capacitive current (A), V is the potential of the electrode (V), and t is the time (s). Usually, the analysis of CV data makes it possible to obtain the value of the effective capacitance, C_{eff}, either by assuming that $\alpha_{dl} = 1$ in Eq. (1) and measuring the current at a given potential, or by using the following integral relation in Eq. (3):

$$C_{eff} = \frac{1}{v(V_f - V_i)} \int_{V_i}^{V_f} i_c(t)\, dV$$

Eq. 3

where, v is the potential scan rate ($V\,s^{-1}$), and V_i and V_f are the potential boundaries of the potential window (V). Both expressions result in the determination of a rate-invariant value of the effective capacitance. At this point, it is worth mentioning that the use of a CPE for the description of the interface provides a mathematical representation of the phenomena, but the physical interpretation of the fractional order of the differential equation is still lacking and under investigation [14,38].

Following the works of Sadkowski [14] and Montella [13], Allagui et al. [15,28,39,40] provided a detailed analysis of the use of CPE in the time domain, and derived an equation allowing to calculate the current from Eq. (4): [15].

$$i_c(t) = Q_{dl} \frac{V_f - V_i}{t_f - Vt_i} \left(\frac{t^{1-\alpha_{dl}}}{\Gamma(2-\alpha_{dl})} - \frac{R_e Q_{dl} t^{1-2\alpha_{dl}}}{\Gamma(2-\alpha_{dl})} + ... \right)$$

Eq. 4

where, Γ is the gamma function.

As with the EIS analysis, the use of Eq. (4) allows for the determination of the two CPE parameters, which in turn must be converted to an effective capacity (the double layer capacitance in the simplest case) using an appropriate model, as explained in the next sections.

The CPE analyzed by impedance

Figure 1b shows the Nyquist representation of the simulated impedance diagrams calculated for a pure capacitance $C_{dl} = 1$ mF and for various value of α_{dl} (Q_{dl} is kept constant at 1 $mFs^{(\alpha_{dl}-1)}$). The shapes of the EIS responses are straight lines, which form an angle with the x-axis whose value depends on α_{dl}. This variation can also be observed on the Bode plot (Figure 1c), in particular the phase angle adjusted from the ohmic drop as a function of the frequency, whose value is $90 \times \alpha_{dl}$ over the entire frequency range [4]. If we determine the capacitance from the value of the imaginary part at a fixed frequency, such as 10 kHz (Figure 1d) as it is often

done in the literature to characterize the capacitive behavior of an electrode [41], the value of the capacity obtained depends on the parameter α_{dl} (red circles in Figure 1d). Assuming that C_{dl} is constant, Brug's formula can be used to evaluate Q_{dl} for different values of α_{dl}, which are then used to calculate impedance diagrams. For an ideally polarizable electrode, the double layer capacitance can be determined from the CPE parameters using the Brug's formula [36] which accounts for a 2D distribution of the impedance over the electrode surface in Eq. (5) [33] under the assumption that the charge transfer resistance is much larger than the electrolyte resistance:

$$C_{eff} = Q_{dl}^{1/\alpha_{dl}} \left(\frac{1}{R_e}\right)^{(1-\alpha_{dl})/\alpha_{dl}} \qquad \text{Eq. 5}$$

The same analysis shows that the capacitance determined at a fixed frequency still depends on the value of α_{dl} (black squares in Figure 1d), and does not allow a precise evaluation of the effective capacitance since it varies between 0.2 and 1 mF depending on the value of α_{dl}. Thus, we conclude that by making the assumption that CPE behavior can be analyzed as an ideal capacitor, a significant error in the determination of C_{eff} occurs.

The CPE analyzed by cyclic voltammetry

Figure 2a shows simulated cyclic voltammograms calculated for a pure capacitor according to Eq. (4) for various scan rates with $C_{dl} = 1$ mF and $R_e = 10\ \Omega$. The shape of the curves is rectangular with the time constants corresponding to the charging and discharging of the capacitor (simulating the EDL) in the presence of the resistor (simulating solution resistance), which is visible after each reversal of the potential sweep direction. As expected, the measured current is proportional to the scan rate, allowing the determination of the experimental effective capacitance, C_{eff}, which is independent of the scan rate.

Figure 2
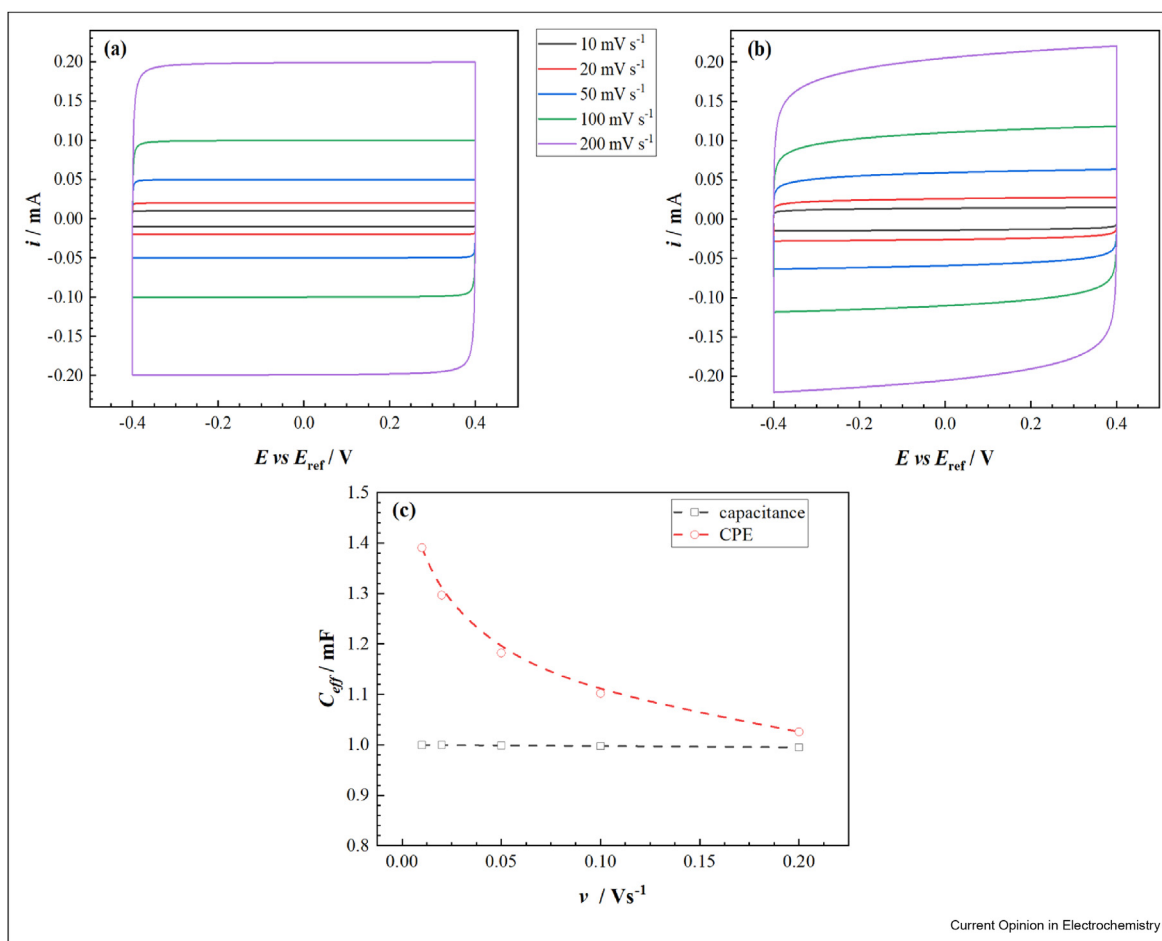
(a) Voltammograms simulated for a pure capacitive behavior of the interface as a function of the scan rate ($C_{dl} = 1$ mF, $R_e = 10\ \Omega$); (b) Voltammograms simulated for a CPE behavior of the interface as a function of the scan rate ($Q_{dl} = 1$ mFs$^{(\alpha_{dl}-1)}$, $\alpha_{dl} = 0.9$, $R_e = 10\ \Omega$); (c) Effective capacitance determined on the CV curves at 0 V vs. E_{ref}.

Figure 2b shows simulated cyclic voltammograms simulated using a CPE in series with a resistor (solution resistance, R_e) according to Eq. (4) for various scan rates with $Q_{dl} = 1\,\mathrm{mFs}^{(\alpha_{dl}-1)}$, $\alpha_{dl} = 0.9$ and $R_e = 10\,\Omega$. The shape of these curves is slightly different from those observed in Figure 2a with an apparent slope of the current/potential trace with respect to the x-axis. The shape of these curves is in agreement with some experimental results reported on a polished gold electrode in 0.1 M perchloric acid solution [42] and for different materials investigated as efficient energy-storage-system [43,44]. It should be noted that this characteristic curve shape can also be observed while

describing the interface of a pure capacitor using a CPE, but occurred due to the presence of a large electrolyte resistance which then gives rise to a non-negligible ohmic drop, but this behavior should not be confused with that of pseudo-capabilities whose origin is different [45,46].

The analysis of the previous CV curves, for example by measuring the current at a potential of 0 V vs. E_{ref}, allows for the evaluation of the interfacial capacitance of the system (Figure 2c). If the CV analysis is performed without taking into account the fact that the interface behaves like a CPE, then the actual value of the

Figure 3
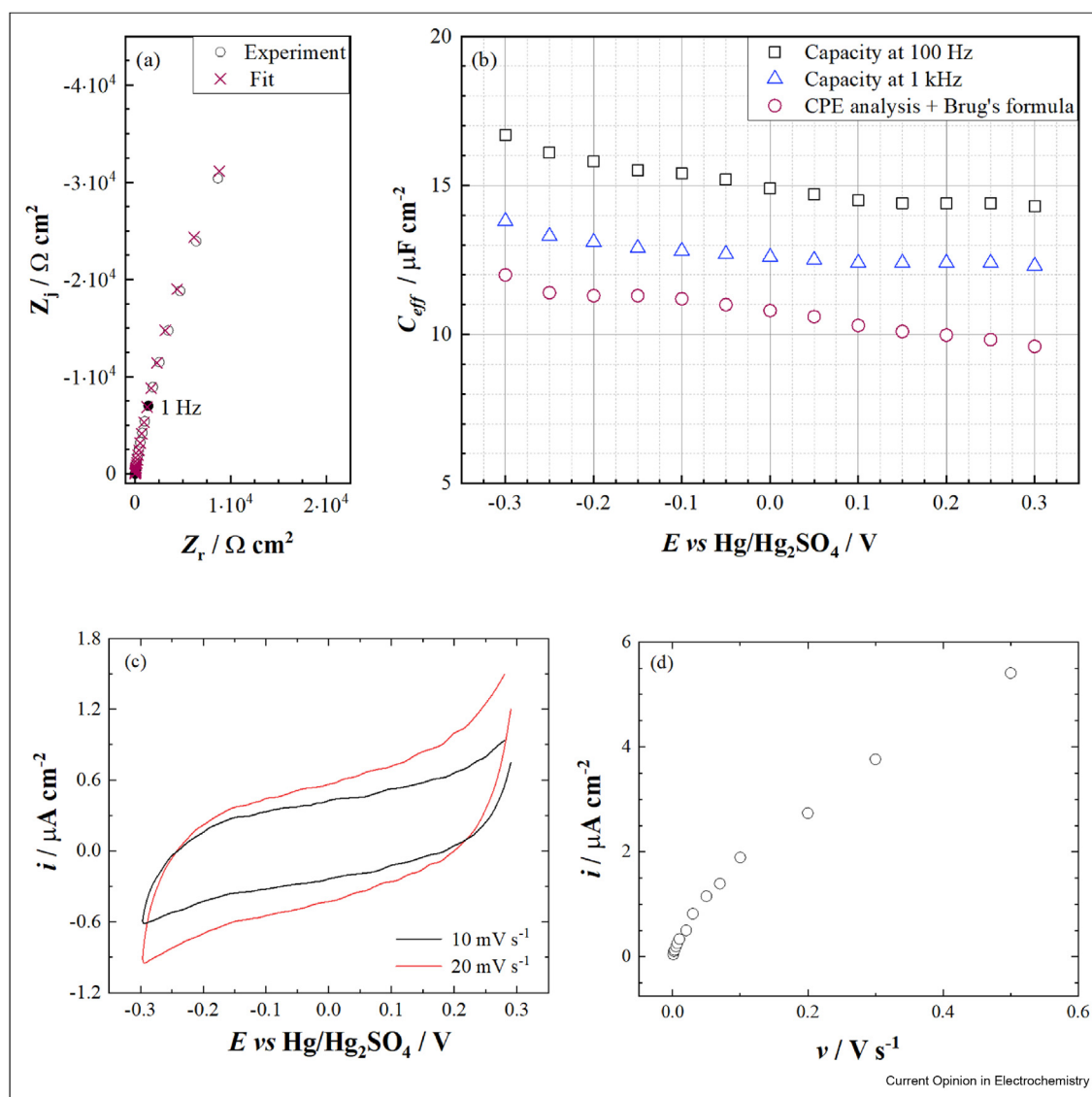
Experiments performed on a gold disk electrode in a sulfuric acid solution (0.1 M) (a) Example of EIS diagram measured –0.10 V/Hg/Hg$_2$SO$_4$; (b) Evaluation of the effective capacitance at 100 Hz, 1 kHz, and using the Brug's formula; (c) Example of CV curves at 10 and 20 mVs^{-1}; (d) Evaluation of the effective capacitance from the capacitive current at 0 V/Hg/Hg$_2$SO$_4$.

capacitance depends on the scan rate at which the measurement is performed. Thus, a value of 1.4 mF for C_{eff} is obtained at 10 mVs^{-1}, while value of 1.03 mF is obtained at 200 mVs^{-1}. For an ideally polarizable electrode, the double layer capacitance can be determined from the CPE parameters using the Brug's formula (Eq. (5)). Using this relationship, the expected effective capacitance is about 600 μF, which is twice as small as the mean value determined by cyclic voltammetry and is independent of the scan rate. Moreover, this analysis relies on the assumption that the CPE parameters are assumed to be independent of the potential during the cyclic voltammetry experiment [42,47,48].

Comparison with experimental results

Figure 3a shows the Nyquist representation of an experimental impedance diagram obtained on a gold electrode in a sulfuric acid solution. The shape of the diagrams is characteristic of CPE behavior as previously discussed for the simulated curves presented in Figure 2. Following the analysis of this impedance response, assuming that it is an ideal capacitor and that we have determined its value at fixed frequency from the imaginary part of the impedance, we obtain values of capacitance that depend on the frequency (Figure 3b). Conversely, if we fit the EIS diagrams with the circuit presented in Figure 1a, we can determine CPE parameters ($Q_{dl} = 28\ \mu Fs^{(\alpha_{dl}-1)}$ and $\alpha_{dl} = 0.918$) and calculate C_{eff} using Brug's formula (Eq. (5)). The variations of C_{eff} presented in Figure 3b show a value in the range of 11 μFcm^{-2} that slightly depends on the potential. A similar study was carried out subsequently with the same experimental setup by cyclic voltammetry (Figure 3c). The shape of the voltammograms is slightly sloped, revealing a CPE behavior, where this shape cannot be attributed to the ohmic drop (small electrolyte resistance and low current). The analysis of the capacitive current at 0 V/Hg/Hg$_2$SO$_4$ shows nonlinear behavior compatible with a CPE (Figure 3d), demonstrating once again that the analysis of these curves requires a realistic description of the interface, such as including a CPE element, otherwise important errors on the determination of the capacity are probable.

However, CPE behavior is not easy to predict. This is due in particular to the fact that the parameters Q and α of the CPE are correlated [35] and it is nowadays often admitted that surface (2D) or volume (3D) distributions of the interface properties result in a CPE behavior. Such behavior can usually be evidenced using graphical analysis [9,49]. Moreover, the purity and cleanliness of the electrode also seem to be important factors, as shown by some experiments performed on hanging or falling mercury drop electrodes (clean renewable surface), or the work of Martin and Lasia on specifically prepared gold electrodes [50]. In these cases, ideal capacitive behaviors were experimentally observed and reported.

Conclusions and perspectives

CPE behaviors are frequently observed in experimental measurements of electrochemical systems supposed to exhibit ideal capacitive responses such as supercapacitors. The consideration and use of a CPE during analysis of experimentally collected electrochemical data is of importance in order to avoid erroneous values of extracted capacitance.

The comparison of interface analysis between EIS vs. CV experiments shows that both techniques allow an accurate evaluation of the interfacial capacitance only when the proper model is used, namely when taking into account a CPE rather than a pure capacitance. It is interesting to note that CPE behavior can be easily identified from EIS and CV representations, but its use to interpret data is common in impedance and not common in voltammetry, which is the technique most often used to characterize supercapacitors.

Declaration of competing interest

The authors declare that they have no known competing financial interests or personal relationships that could have appeared to influence the work reported in this paper.

Data availability

Data will be made available on request.

References

Papers of particular interest, published within the period of review, have been highlighted as:

* * of special interest
* ** of outstanding interest

1. Budkov YA, Kolesnikov AL: **Electric double layer theory for room temperature ionic liquids on charged electrodes: milestones and prospects**. *Curr Opin Electrochem* 2022, **33**.

2. Sebastián-Pascual P, Shao-Horn Y, Escudero-Escribano M: **Toward understanding the role of the electric double layer structure and electrolyte effects on well-defined interfaces for electrocatalysis**. *Curr Opin Electrochem* 2022, **32**.

3. Shin SJ, Kim DH, Bae G, Ringe S, Choi H, Lim HK, Choi CH, Kim H: **On the importance of the electric double layer structure in aqueous electrocatalysis**. *Nat Commun* 2022, **13**:174.

4. Orazem ME, Tribollet B: *Electrochemical impedance spectroscopy*. 2nd ed. Hoboken, New Jersey: Wiley; 2017.

5. Helseth LE: **Comparison of methods for finding the capacitance of a supercapacitor**. *J Energy Storage* 2021, **35**.

6. Kurzweil P, Schottenbauer J, Schell C: **Past, present and future of electrochemical capacitors: pseudocapacitance, aging mechanisms and service life estimation**. *J Energy Storage* 2021, **35**.

7. Ge Y, Xie X, Roscher J, Holze R, Qu Q: **How to measure and report the capacity of electrochemical double layers, supercapacitors, and their electrode materials**. *J Solid State Electrochem* 2020, **24**:3215−3230.

8. Wang S, Zhang J, Gharbi O, Vivier V, Gao M, Orazem ME: **Electrochemical impedance spectroscopy**. *Nat Rev Methods Primers* 2021, **1**:41.

9. Vivier V, Orazem ME: **Impedance analysis of electrochemical systems**. *Chem Rev* 2022, **122**:11131−11168.

10. Láng G, Heusler KE: **Remarks on the energetics of interfaces exhibiting constant phase element behaviour**. *J Electroanal Chem* 1998, **457**:257−260.

11. Zoltowski P: **On the electrical capacitance of interfaces exhibiting constant phase element behaviour**. *J Electroanal Chem* 1998, **443**:149−154.

12. Lasia A: **The origin of the constant phase element**. *J Phys Chem Lett* 2022, **13**:580−589.

13. Montella C: **LSV/CV modelling of electrochemical reactions with interfacial CPE behaviour, using the generalised Mittag-Leffler function**. *J Electroanal Chem* 2012, **667**:38−47.

14. Sadkowski A: **Time-domain responses of constant phase electrodes**. *Electrochim Acta* 1993, **38**:2051−2054.

15. Allagui A, Freeborn TJ, Elwakil AS, Maundy BJ: **Reevaluation of performance of electric double-layer capacitors from constant-current charge/discharge and cyclic voltammetry**. *Sci Rep* 2016, **6**, 38568.

16. Gharbi O, Tran MTT, Tribollet B, Turmine M, Vivier V: **Revisiting cyclic voltammetry and electrochemical impedance spectroscopy analysis for capacitance measurements**. *Electrochim Acta* 2020, **343**, 136109.
*
In this article, a comprehensive discussion on the determination of the effective capacitance of electrified interface is presented based on CV and EIS experiments.

17. Scisco GP, Orazem ME, Ziegler KJ, Jones KS: **On the rate capability of supercapacitors characterized by a constant-phase element**. *J Power Sources* 2021, **516**.
* *
The authors provide a detailed analyis of CV curves and EIS diagrams obtained on supercapacitors and analyzed numerous experimental results from the literature.

18. Marcelin S, Zhang Z, Ter-Ovanessian B, Normand B: **Relationship between the resistivity profiles obtained from the power law model and the physico-chemical properties of passive films**. *J Electrochem Soc* 2021, **168**.

19. Gomes MP, Costa I, Pébère N, Rossi JL, Tribollet B, Vivier V: **On the corrosion mechanism of Mg investigated by electrochemical impedance spectroscopy**. *Electrochim Acta* 2019, **306**:61−70.

20. Roggero A, Caussé N, Dantras E, Villareal L, Santos A, Pébère N: **Thermal activation of impedance measurements on an epoxy coating for the corrosion protection: 2. electrochemical impedance spectroscopy study**. *Electrochim Acta* 2019, **305**:116−124.

21. Margarit-Mattos ICP: **EIS and organic coatings performance: revisiting some key points**. *Electrochim Acta* 2020, **354**, 136725.

22. Miszczyk A, Darowicki K: **Water uptake in protective organic coatings and its reflection in measured coating impedance**. *Prog Org Coating* 2018, **124**:296−302.

23. Lai X, He L, Wang S, Zhou L, Zhang Y, Sun T, Zheng Y: **Co-estimation of state of charge and state of power for lithium-ion batteries based on fractional variable-order model**. *J Clean Prod* 2020:255.

24. Chen N, Zhang P, Dai J, Gui W: **Estimating the state-of-charge of lithium-ion battery using an H-infinity observer based on electrochemical impedance model**. *IEEE Access* 2020, **8**:26872−26884.

25. Xu J, Mi CC, Cao B, Cao J: **A new method to estimate the state of charge of lithium-ion batteries based on the battery impedance model**. *J Power Sources* 2013, **233**:277−284.

26. Huang J, Gao Y, Luo J, Wang S, Li C, Chen S, Zhang J: **Impedance response of porous electrodes: theoretical framework, physical models and applications**. *J Electrochem Soc* 2020, **167**.

27. Cheng C-S, Chung HS-H, Lau RW-H, Hong KY-W: **Time-domain modeling of constant phase elements for simulation of lithium battery behavior**. *IEEE Trans Power Electron* 2019, **34**:7573−7587.

28. Allagui A, Freeborn TJ, Elwakil AS, Fouda ME, Maundy BJ, Radwan AG, Said Z, Abdelkareem MA: **Review of fractional-order electrical characterization of supercapacitors**. *J Power Sources* 2018, **400**:457−467.

29. Hernández-Balaguera E, Arredondo B, Pozo Gd, Romero B: **Exploring the impact of fractional-order capacitive behavior on the hysteresis effects of perovskite solar cells: a theoretical perspective**. *Commun Nonlinear Sci Numer Simulat* 2020, **90**.

30. Tolouei NE, Ghamari S, Shavezipur M: **Development of circuit models for electrochemical impedance spectroscopy (EIS) responses of interdigitated MEMS biochemical sensors**. *J Electroanal Chem* 2020:878.

31. Yavarinasab A, Janfaza S, Tasnim N, Tahmooressi H, Dalili A, Hoorfar M: **Graphene/poly (methyl methacrylate) electrochemical impedance-transduced chemiresistor for detection of volatile organic compounds in aqueous medium**. *Anal Chim Acta* 2020, **1109**:27−36.

32. Wang H, Pilon L: **Intrinsic limitations of impedance measurements in determining electric double layer capacitances**. *Electrochim Acta* 2012, **63**:55−63.

33. Hirschorn B, Orazem ME, Tribollet B, Vivier V, Frateur I, Musiani M: **Determination of effective capacitance and film thickness from constant-phase-element parameters**. *Electrochim Acta* 2010, **55**:6218−6227.

34. Córdoba-Torres P: **Relationship between constant-phase element (CPE) parameters and physical properties of films with a distributed resistivity**. *Electrochim Acta* 2017, **225**:592−604.

35. Córdoba-Torres P, Mesquita TJ, Devos O, Tribollet B, Roche V, Nogueira RP: **On the intrinsic coupling between constant-phase element parameters α and Q in electrochemical impedance spectroscopy**. *Electrochim Acta* 2012, **72**:172−178.

36. Brug GJ, Vandeneeden ALG, Sluytersrehbach M, Sluyters JH: **The analysis of electrode impedances complicated by the presence of a constant phase element**. *J Electroanal Chem* 1984, **176**:275−295.

37. Holm S, Holm T, Martinsen OG: **Simple circuit equivalents for the constant phase element**. *PLoS One* 2021, **16**, e0248786.

38. Czuczwara W, Latawiec KJ, Stanisɫawski R, Łukaniszyn M, Kopka R, Rydel M: **Modeling of a supercapacitor charging circuit using two equivalent RC circuits and forward vs. Backward fractional-order differences, 2018**. *Prog Appl Electr Eng* 2018:1−6 (PAEE).

39. Allagui A, Alnaqbi H, Elwakil AS, Said Z, Hachicha AA, Wang CL, Abdelkareem MA: **Fractional-order electric double-layer capacitors with tunable low-frequency impedance phase angle and energy storage capabilities**. *Appl Phys Lett* 2020, **116**.

40. Fouda ME, Allagui A, Elwakil AS, Eltawil A, Kurdahi F: **Supercapacitor discharge under constant resistance, constant current and constant power loads**. *J Power Sources* 2019:435.
* *
In this article, both theoretical and experimental approches are used to study the discharge response of supercapacitors. It is shown that a better descritpion of the system is obtained when using a CPE element instead of a pure capacitor.

41. Harrington SP, Devine TM: **Analysis of electrodes displaying frequency dispersion in Mott-Schottky tests**. *J Electrochem Soc* 2008, **155**:C381−C386.

42. Schalenbach M, Durmus YE, Tempel H, Kungl H, Eichel RA: **Double layer capacitances analysed with impedance spectroscopy and cyclic voltammetry: validity and limits of the**

constant phase element parameterization. *Phys Chem Chem Phys* 2021, **23**:21097−21105.

43. Simon P, Gogotsi Y: **Perspectives for electrochemical capacitors and related devices**. *Nat Mater* 2020, **19**: 1151−1163.

44. Park H, Ambade RB, Noh SH, Eom W, Koh KH, Ambade SB, Lee WJ, Kim SH, Han TH: **Porous graphene-carbon nanotube scaffolds for fiber supercapacitors**. *ACS Appl Mater Interfaces* 2019, **11**:9011−9022.

45. Costentin C: **Electrochemical energy storage: questioning the**
 * **popular v/v(1/2) scan rate diagnosis in cyclic voltammetry**. *J Phys Chem Lett* 2020, **11**:9846−9849.
In this article, an interesting discussion on the use of v/v1/2 scan rate diagnosis is provided and shown to be usually wrong.

46. Costentin C, Porter TR, Saveant JM: **How do pseudocapacitors store energy? Theoretical analysis and experimental illustration**. *ACS Appl Mater Interfaces* 2017, **9**:8649−8658.

47. Charoen-amornkitt P, Suzuki T, Tsushima S: **Effects of voltage-dependence of the constant phase element and ohmic parameters in the modeling and simulation of cyclic voltammograms**. *J Electrochem Soc* 2020, **167**.

48. Schalenbach M, Durmus YE, Tempel H, Kungl H, Eichel R-A:
 * **A dynamic transmission line model to describe the potential dependence of double-layer capacitances in cyclic voltammetry**. *J Phys Chem C* 2021, **125**:27465−27471.
The objective of this study is to provide a comprehensive description on the influence of the potential on the capacitive response of an electrode measured by cyclic voltammetry.

49. Orazem ME, Pebere N, Tribollet B: **Enhanced graphical representation of electrochemical impedance data**. *J Electrochem Soc* 2006, **153**:B129−B136.

50. Martin MH, Lasia A: **Influence of experimental factors on the constant phase element behavior of Pt electrodes**. *Electrochim Acta* 2011, **56**:8058−8068.